

copy 2



RESEARCH MEMORANDUM

EXPERIMENTAL INVESTIGATION OF THRUST AUGMENTATION
OF A TURBOJET ENGINE AT ZERO RAM BY
MEANS OF TAIL-PIPE BURNING

By Bruce T. Lundin, Harry W. Dowman, and David S. Gabriel
Aircraft Engine Research Laboratory
Cleveland, Ohio

CLASSIFIED DOCUMENT

This document contains classified information affecting the National Defense of the United States within the meaning of the Espionage Act, USC 50:31 and 32. Its transmission or the revelation of its contents in any manner to an unauthorized person is prohibited by law. Information so classified may be imparted only to persons in the military and naval Services of the United States, appropriate civilian officers and employees of the Federal Government who have a legitimate interest therein, and to United States citizens of known loyalty and discretion who of necessity must be informed thereof.



NATIONAL ADVISORY COMMITTEE FOR AERONAUTICS

WASHINGTON
January 6, 1947

NACA LIBRARY
RECEIVED
JAN 14 1947

CLASSIFICATION CANCELLED

Authority *J.W. Crowley*
Date *12/14/53*
By *219/514*
See 219/514
27-2208

~~CONFIDENTIAL~~

UNCLASSIFIED



UNCLASSIFIED

NATIONAL ADVISORY COMMITTEE FOR AERONAUTICS

RESEARCH MEMORANDUM

EXPERIMENTAL INVESTIGATION OF THRUST AUGMENTATION OF A TURBOJET

ENGINE AT ZERO RAM BY MEANS OF TAIL-PIPE BURNING

By Bruce T. Lundin, Harry W. Dowman, and David S. Gabriel

SUMMARY

The performance of a turbojet engine equipped with a tail-pipe burner designed by the NACA has been investigated at zero ram over a range of rotor speeds and tail-pipe-burner fuel flows. The burner is simple in construction, consisting essentially of an enlarged tail pipe incorporating fuel-spray nozzles and a flame holder. An adjustable-area exhaust nozzle is installed at the burner discharge.

A thrust augmentation of 40 percent was obtained at zero ram for a tail-pipe-burner fuel-air ratio of 0.043 or a total fuel-air ratio of 0.056. The over-all specific fuel consumption for this thrust increase was about 3.1 pounds per hour per pound of thrust. These tests were conducted with turbine-discharge pressures lower than normal and therefore slightly higher thrust augmentations would be expected under rated engine operating conditions. Calculations of engine and burner performance at ram conditions, based on the test data, indicate a net-thrust augmentation of 140 percent at a flight speed of 900 miles per hour.

Although the maximum tail-pipe-burner discharge temperatures were estimated at about 4000° R, the temperature of the burner shell and adjustable nozzle did not exceed 1200° F for any test. This condition obviated the need for any special cooling of the burner shell.

The loss in thrust without afterburning caused by the internal drag of the tail-pipe burner was 6.7 percent for a test condition with oversized exhaust-nozzle area and therefore lower than rated turbine-discharge pressure and temperature. Calculations show that this value would be reduced to about $3\frac{1}{2}$ percent at rated engine conditions.

~~CONFIDENTIAL~~

UNCLASSIFIED

INTRODUCTION

The inherently low propulsive efficiency of turbojet engines at low flight speeds results in relatively poor take-off and climb characteristics of jet-propelled aircraft as compared with conventional engine-propeller powered aircraft. In order to improve the low-speed flight characteristics of jet-propelled aircraft, it is necessary to augment the normal engine thrust for short periods of time. The availability of momentary thrust augmentation is particularly desirable for military aircraft in order to obtain the additional thrust required for high-speed flight.

An investigation of various methods of augmenting the thrust of turbojet engines is being conducted at the NACA Cleveland laboratory. One of the methods being investigated is tail-pipe burning, or afterburning, wherein the gas temperatures and jet velocities are increased by the burning of additional fuel in the tail pipe of the engine. This method of thrust augmentation is particularly advantageous because of the ease of operation and relatively low liquid consumption as compared with other methods. Because only a small amount of additional equipment is required for the tail-pipe-burner installation, which consists mainly of an adjustable-area exhaust nozzle and enlarged tail pipe incorporating fuel nozzles and a flame holder, this method also has the practical advantage of simplicity of installation.

A wind-tunnel investigation of a turbojet engine equipped with a tail-pipe burner, which was conducted under various flight and altitude conditions, is described in reference 1. A concurrent investigation of the performance of various other types of tail-pipe burner was conducted at zero ram and sea-level conditions. The tail-pipe burner incorporating the most satisfactory design features investigated and the performance of a turbojet engine equipped with this burner are described. This performance investigation covered a range of rotor speeds and tail-pipe-burner fuel flows. The results are compared with the performance of the engine with the standard tail pipe and the effect of the tail-pipe burner without afterburning on the thrust of the engine is evaluated.

APPARATUS

Test engine. - The performance of the tail-pipe burner was investigated on a TG-180 turbojet engine, which has an 11-stage axial-flow compressor, eight cylindrical combustion chambers, and a single-stage turbine. The rating of the engine is as follows:

Static thrust, pounds	4000
Rotor speed, rpm	7700
Tail-pipe gas temperature, °R	1660

For all tests, JP-1 fuel was used in the engine and AN-F-22 fuel was used in the tail-pipe burner.

Engine installation. - The general arrangement of the installation of the engine with the standard tail pipe is shown in figure 1. A spherical "clam-shell" type adjustable-area exhaust nozzle having a discharge-area range from 224 to 283 square inches was installed at the end of a 30-inch long tail pipe. This short tail pipe, which has an inside diameter of 21 inches, was installed to provide for discharge of the exhaust gas outside the test cell. The engine was mounted on a swinging framework suspended from the ceiling of the test cell and the engine thrust was balanced and measured with an air-pressure diaphragm (fig. 1). An inlet-air nozzle, fitted with an exit diffuser, was used to determine the air flow. The engine speed and fuel flows were measured with standard instrumentation.

Tail-pipe burner. - Several different types of tail-pipe burner were investigated; the complete assembly of the engine with the burner that incorporated the most satisfactory design features is shown in figure 2. This burner is simple in construction, consisting essentially of an enlarged tail pipe, which incorporates fuel-spray nozzles and a flame holder. A sketch of the tail-pipe burner showing the details of construction is shown in figure 3; a photograph of the burner assembly removed from the engine is shown in figure 4.

The burner shell consists of a 6-foot section of straight duct made out of one-sixteenth inch thick Inconel and has an inside diameter of $25\frac{3}{4}$ inches. The burner is attached to the engine by means of an annular diffuser section having an outlet-to-inlet area ratio of 1.5 and a short adapter section, which is bolted to the turbine-discharge flange (fig. 3). The annular diffuser is formed by an inner cone, similar to but slightly shorter than the standard turbine-discharge inner cone, and an outer duct. An adjustable-area exhaust nozzle similar to that used in the standard tail pipe and with a discharge-area range from 265 to 397 square inches is fitted to the discharge of the tail-pipe burner.

As shown in figure 3, the fuel was introduced into the tail-pipe burner through two rings of spray nozzles, an upstream ring and a downstream ring. The upstream spray-nozzle ring protrudes about one-eighth inch from the surface of the turbine-discharge inner cone near the turbine discharge and consists of twenty 40-gallon-per-hour

nozzles. The downstream nozzle ring consists of eighteen 60-gallon-per-hour spray nozzles located within the tail-pipe burner near the end of the turbine-discharge inner cone. The spray nozzles in this second ring, which has a diameter of $14\frac{1}{2}$ inches, were directed downstream. A small step in the turbine-discharge inner cone provided a seat for the flame produced by the fuel injected from the upstream ring of nozzles. A 2 inch wide, semitoroidal flame holder having a diameter of 16 inches was located approximately 9 inches downstream of the downstream ring of spray nozzles. A photograph of the adapter section and the modified turbine-discharge inner cone, showing the upstream ring of fuel nozzles, is presented in figure 5. A photograph of the tail-pipe-burner section, including the downstream fuel nozzles and flame holder, viewed from the upstream end is shown in figure 6. A single spark plug located near the step in the turbine-discharge inner cone was provided for ignition.

Temperature and pressure instrumentation. - The stations at which the engine with the standard tail pipe and the tail-pipe burner were instrumented for temperature and pressure measurements are shown in figures 1 and 2, respectively.

The number, type, and location of thermocouples were as follows:

(a) Total temperature at compressor inlet (station 1) T_1 : average of 20 thermocouples, five in each of four rakes 90° apart in the inlet annulus.

(b) Indicated gas temperature at turbine discharge (station 5) T_5 : average of eight strut-type thermocouples located approximately 4 inches downstream of the turbine discharge, $1\frac{1}{2}$ inches in from the duct wall, and on the center line of each of the eight combustion chambers.

(c) Gas temperature at standard tail-pipe inlet (station 6) T_6 : average of eight strut-type thermocouples equally spaced in a circle 4 inches in from the tail-pipe wall.

The number, type, and location of pressure tubes were as follows:

(a) Total pressure at compressor inlet (station 1) P_1 : average of eight total-pressure tubes, two in each of four rakes 90° apart (check provided by open-end tube in quiet zone of test cell).

(b) Static pressure at tail-pipe-burner inlet (station 6) p_6 : pressure of piezometer ring connected to four equally spaced wall taps.

(c) Static pressure at tail-pipe-burner outlet (station 7) p_7 : pressure of piezometer ring connected to four equally spaced wall taps.

Four thermocouples were also spot-welded to the shell of the tail-pipe burner and to the adjustable-area exhaust nozzle at the locations shown in figure 2.

PROCEDURE

The following tests were conducted to determine the performance and operating characteristics of the engine equipped with the tail-pipe burner:

Test A. - Engine performance tests using the standard tail pipe were conducted for four positions of the adjustable-area exhaust nozzle over a range of indicated rotor speeds from 6000 to 7700 rpm.

Test B. - Performance tests of the engine equipped with the tail-pipe burner were run for a range of total tail-pipe-burner fuel flows from 1.0 to 3.0 pounds per second and over a range of indicated rotor speeds from 6500 to 7700 rpm. The position of the adjustable-area exhaust nozzle was varied as required to maintain the turbine-discharge temperatures within the range of those obtained in the tests with the standard tail pipe. For each total tail-pipe-burner fuel flow, the proportion of fuel injected in the upstream and downstream fuel manifolds was varied within the range of satisfactory burner operation.

Test C. - Performance tests of the engine equipped with the tail-pipe burner were conducted without afterburning, with the adjustable nozzle in the closed position, and over a range of rotor speeds from 6000 to 7700 rpm. This test was conducted to evaluate the loss in engine thrust without afterburning caused by the internal drag of the tail-pipe burner.

Test D. - Test A was repeated to determine the change in standard-engine performance that occurred during the tail-pipe-burner and drag tests.

No special effort was made in any of these tests to provide an ignition system that would ignite the tail-pipe burner at high engine speeds. With the burner ignition system used it was necessary to reduce the rotor speed to approximately 4000 rpm before igniting the burner.

SYMBOLS

The following symbols are used in this report:

F	thrust of engine with standard tail pipe, (lb)
F_b	thrust of engine with tail-pipe burner, (lb)
f	total specific fuel consumption for engine and tail-pipe burner, (lb)/(hr)(lb thrust)
$(f/a)_b$	tail-pipe-burner fuel-air ratio
N	rotor speed, (rpm)
P	total pressure, (lb/sq in. absolute)
p	static pressure, (lb/sq in. absolute)
q_b	tail-pipe-burner inlet velocity pressure (based on average velocity computed for section 6-6, fig. 2), (lb/sq ft absolute)
T	total (indicated) gas temperature, ($^{\circ}R$)
W_a	air flow, (lb/sec)
$W_{f,b}$	fuel flow to tail-pipe burner, (lb/sec)
$W_{f,e}$	fuel flow to engine, (lb/hr)
Δp_f	friction static-pressure drop between stations 6-6 and 7-7 (fig. 2), (lb/sq ft absolute)
δ	ratio of compressor-inlet total pressure P_1 to NACA standard sea-level pressure
θ	ratio of compressor-inlet total temperature T_1 to NACA standard sea-level temperature

Subscripts:

1	compressor inlet
5	turbine discharge
6	tail-pipe-burner inlet (or tail pipe)
7	tail-pipe-burner outlet

METHOD OF CORRECTION AND DATA ANALYSIS

All engine performance data are corrected to standard conditions at the compressor inlet by means of the following correction factors:

$f/\sqrt{\theta}$	corrected total specific fuel consumption, (lb)/(hr)(lb thrust)
F/δ	corrected thrust, (lb)
$N/\sqrt{\theta}$	corrected rotor speed, (rpm)
T/θ	corrected temperature, ($^{\circ}$ R)
$\frac{W_{a,\theta}}{\delta}$	corrected air flow, (lb/sec)
$\frac{W_{f,e}}{\delta\sqrt{\theta}}$	corrected fuel flow to engine, (lb/hr)
$\frac{W_{f,b}}{\delta\sqrt{\theta}}$	corrected fuel flow to tail-pipe burner, (lb/sec)

The fuel flow to the tail-pipe burner $W_{f,b}$ is corrected in the same manner as the engine fuel flow $W_{f,e}$ in order to keep the same tail-pipe-burner temperature ratio, hence the same thrust augmentation, over the range of the correction.

The engine thrust obtained with the tail-pipe burner should be compared with the thrust obtained with the standard tail pipe at the same corrected rotor speed and turbine-discharge gas temperature. Because of the possibility that differences in the thermocouple locations and the tail-pipe design for the two configurations might cause the use of measured turbine-discharge temperatures to result in an unreliable comparison of engine performance, the corrected engine fuel flow was used as the reference parameter. For each test point with tail-pipe burning, the exhaust-nozzle size for the standard engine that resulted in the same corrected engine fuel flow (at the same corrected speed) was determined from the curves of test D and the corresponding thrust of the engine with the standard tail pipe determined for this nozzle size. Because the turbine-discharge temperature for both configurations would be the same at the same corrected rotor speed and engine fuel flow if the component efficiencies of the engine did not change, the comparison of engine thrust obtained in this manner is effectively made at the same rotor speed and turbine-discharge gas temperature.

RESULTS AND DISCUSSION

Engine with Standard Tail Pipe

The thrust of the engine with the standard tail pipe at a corrected rotor speed of 7500 rpm for tests A and D is shown plotted against the corrected fuel flow to the engine in figure 7. These data were obtained from cross plots of engine thrust against rotor speed for the different positions of the adjustable-area exhaust nozzle and show that the change in engine thrust during tests B and C is very small. Because of this small change in engine thrust, the performance of the engine with the standard tail pipe may be obtained from either test A or D. Accordingly, the results of test D are used as a basis for evaluation of tests B and C.

The performance of the engine with the standard tail pipe (obtained from test D) is shown in figure 8, in which corrected thrust, fuel flow, turbine-discharge gas temperature, tail-pipe gas temperature, and air flow are plotted against the corrected rotor speed. The turbine-discharge temperature T_5 is about 100°F higher than the tail-pipe gas temperature T_6 because it was measured by thermocouples located in a hot region of a circumferentially unoven temperature field at the turbine discharge. During tests with both the standard tail pipe (tests A and D) and with the tail-pipe burner (test B), the engine was operated with tail-pipe gas temperatures approximately 100°F below normal in order to prolong the engine life. The increased exhaust-nozzle area required to maintain these lower temperatures resulted in lower pressures with approximately the same gas velocity at the inlet to the tail-pipe burner as compared with rated engine operation. Because these changes in temperature and pressure are considered adverse to combustion, this test procedure is considered conservative insofar as the combustion characteristics of the tail-pipe burner are concerned. These lower tail-pipe-burner inlet pressures would also result in slightly lower thrust augmentation for the same burner temperature ratio, as will be illustrated later.

Engine with Tail-Pipe Burner, No Afterburning

A comparison of the performance of the engine with the tail-pipe burner without afterburning (test C) to the engine performance with the standard tail pipe (test D) is shown in figure 9. For this comparison, the performance of the engine with the standard tail pipe is given for the same engine fuel flows as obtained with the tail-pipe burner. The engine thrust for both of these tests is lower than the maximum obtained in test D (fig. 8(a)) because the minimum area of

the burner tail-pipe nozzle was too large to permit operation without afterburning at desired turbine-discharge gas temperatures. A comparison of tests C and D shows that the tail-pipe burner causes a loss in thrust of about 6.7 percent (200 lb) at a corrected rotor speed of 7700 rpm (fig. 9(a)). Because of the lower pressures in the tail pipe caused by the oversized exhaust nozzle, this loss in thrust is higher than would be obtained if the engine were operated at rated conditions. Theoretical calculations based on this measured thrust loss at the conditions of the test indicate that a loss of thrust of about $3\frac{1}{2}$ percent would occur if the exhaust-nozzle area were sufficiently reduced to maintain maximum allowable gas temperatures. As would be expected, both the tail-pipe gas temperatures and the air flow are only slightly affected by the installation of the tail-pipe burner.

The friction pressure-drop coefficient $\Delta p_f/q_b$ of the tail-pipe burner was determined from the measured static-pressure drop between the burner inlet and the burner outlet and had a constant value of about 0.30 over the range of the tests. Although this pressure-drop coefficient is considered only approximate because of the difficulty of accurately measuring the small difference in pressure, it indicates that the internal drag of the burner is low.

Engine with Tail-Pipe Burner, Afterburning

Engine performance. - The corrected performance of the engine with afterburning over a range of rotor speeds and for various fuel flows into the tail-pipe burner (test B) is presented in table I.

The ratio of the thrust obtained with the tail-pipe burner to the thrust obtained with the standard tail pipe at a corrected rotor speed of 7500 rpm (indicated rotor speed, approximately 7700 rpm) is plotted against the ratio of tail-pipe-burner fuel-air ratio to turbine-discharge gas temperature $(f/a)_b/T_5$ in figure 10. When the effects of dissociation and variable specific heats are neglected, the factor $(f/a)_b/T_5$ is proportional to the tail-pipe-burner temperature ratio and therefore serves to correlate the data. A maximum increase in thrust of 40 percent was obtained, at which point the corrected tail-pipe-burner fuel-air ratio was 0.043 (total fuel-air ratio, 0.056) and the corrected turbine-discharge gas temperature was 1600° R. The scatter of the data is attributed mainly to variations in tail-pipe-burner efficiency and also in part to variations in turbine-discharge pressure between the various test points. Although a superficial examination of the data may indicate that highest thrust augmentation is obtained when 50 to 60 percent of

the fuel is injected in the upstream fuel nozzles, the effect of the variation in turbine-discharge pressures would obscure any effect of the fuel-injection method on the thrust augmentation. The effect of the method of fuel injection on the operating characteristics of the tail-pipe burner is subsequently discussed.

A plot of the thrust augmentation as a function of the total specific fuel consumption is presented in figure 11 for a corrected rotor speed of approximately 7500 rpm. This curve shows that the total specific fuel consumption increases from about 1.1 to 3.1 pounds per hour per pound of thrust as the augmentation increases from 0 to 40 percent. The scatter of the test points is attributed mainly to variations in tail-pipe-burner and turbine-discharge pressures, as was noted in figure 10 and, to a lesser extent, to changes in the turbine-discharge temperatures.

The thrust augmentation is replotted as a function of the ratio of tail-pipe-burner outlet temperature to inlet temperature in figure 12. The theoretical thrust augmentation for both rated turbine-discharge conditions and the average conditions obtained during test B is included for comparison. The calculations for these theoretical curves were based on the internal drag of the tail-pipe burner as determined from the measured thrust loss of test C. It is noted from these theoretical curves that the thrust augmentation for any fixed temperature ratio is higher for rated engine conditions than for the average conditions of the tests. This difference is mainly due to the smaller effect of burner pressure drop at the higher burner-inlet pressures attendant with rated engine operation. From these considerations, it may be expected that thrust augmentations greater than 40 percent would be obtained with the present tail-pipe burner at rated engine operating conditions.

The temperature ratio for each of the test points was calculated from the measured tail-pipe-burner fuel-air ratio and turbine-discharge temperature, including the effects of dissociation and variable specific heats. Although a high degree of accuracy cannot be claimed for calculations of temperature ratio at rich mixtures, the good agreement between the theoretical curve (for the test conditions) and the test points indicates that the over-all efficiency of the tail-pipe burner was high.

Because both the propulsive efficiency of the engine and the turbine-discharge pressure increase with flight speed, the net-thrust augmentation for any fixed tail-pipe-burner temperature ratio also increases as the flight speed is raised. This characteristic is illustrated in figure 13 in which the calculated net-thrust augmentation is plotted against flight speed in miles per hour for sea-level

conditions. A scale of corresponding flight Mach numbers is included for convenience. Curves for both rated engine operating conditions and for the turbine-discharge conditions obtained for the test point at the highest tail-pipe-burner fuel flow are presented in this figure. The variation of engine operating conditions with flight speed was determined from calculations based on the performance curves of figure 8 and the thrust augmentation was calculated by theoretical methods. Both of the curves were calculated for a constant temperature-rise ratio of 2.34; this temperature ratio is the ratio required to obtain a thrust augmentation of 40 percent at zero ram for the conditions of the chosen test point. The tail-pipe gas temperature was assumed to be held constant (at 1475° R for test conditions and 1660° R for rated conditions) over the range of flight speeds by adjustment of the exhaust-nozzle area.

No combustion difficulty would be expected with the tail-pipe burner at high flight speeds because of the considerable increase in burner-inlet pressure which, as was noted previously, is favorable to combustion. The burner fuel-air ratio would, of course, be constant over the range of flight speeds because the tail-pipe gas temperature was assumed constant. The curve calculated from actual test conditions indicates that a thrust augmentation of 140 percent may be expected at 900 miles per hour (ram-pressure ratio, 2.11 at sea level).

Operating characteristics. - In general, the most satisfactory operation of the tail-pipe burner was obtained when an equal or slightly greater quantity of fuel was injected in the upstream fuel nozzles than in the downstream fuel nozzles. The injection of greater quantities of fuel in the downstream fuel nozzles resulted in reduced thrust augmentation and overheating of the burner shell. When more than 60 percent of the fuel was injected from the upstream spray nozzles, the combustion became rough and intermittent. Steady combustion was obtained throughout the range of test conditions presented.

Although the maximum tail-pipe-burner outlet temperatures are estimated at about 4000° R, the temperature measured on both the burner shell and exhaust nozzle did not exceed 1200° F for any of the tests reported. This condition, which is attributed to a layer of low-temperature gas along the inside of the burner wall, obviated the need for any special cooling of the tail-pipe-burner shell.

SUMMARY OF RESULTS

An investigation of thrust augmentation at zero ram conducted on a turbojet engine equipped with a simple tail-pipe burner designed by the NACA gave the following results:

1. A thrust augmentation of 40 percent was obtained at zero ram for a tail-pipe-burner fuel-air ratio of 0.043, or a total fuel-air ratio of 0.056. The over-all specific fuel consumption for this thrust increase was about 3.1 pounds per hour per pound of thrust. These tests were conducted with turbine-discharge pressures lower than normal and therefore slightly higher thrust augmentations would be expected under rated engine operating conditions. Calculations of engine and burner performance at ram conditions, based on the test data, indicated a net-thrust augmentation of 140 percent at 900 miles per hour.

2. Although the maximum tail-pipe-burner discharge temperatures were estimated at about 4000° R, the temperature of the burner shell and adjustable nozzle did not exceed 1200° F for any test. This condition obviated the need for any special cooling of the burner shell.

3. The loss in thrust without afterburning caused by the internal drag of the tail-pipe burner was 6.7 percent for a test condition with oversized exhaust-nozzle area and therefore lower than rated

turbine-discharge pressure and temperature. Calculations show that this value would be reduced to about $3\frac{1}{2}$ percent at rated engine conditions.

Aircraft Engine Research Laboratory,
National Advisory Committee for Aeronautics,
Cleveland, Ohio.

REFERENCE

1. Fleming, W. A., and Dietz, R. O.: Altitude-Wind-Tunnel Investigations of Thrust Augmentation of a Turbojet Engine.
I - Performance with Tail-Pipe Burning. NACA RM No. E6I20, 1946.

TABLE I - CORRECTED PERFORMANCE DATA FOR TAIL-PIPE-BURNING TESTS, TEST B

Run	Rotor speed (rpm)	Thrust (lb)	Engine fuel flow (lb/hr)	Air flow (lb/sec)	Turbine-discharge temperature (°R)	Tail-pipe-burner fuel flow			Tail-pipe-burner fuel-air ratio	Total fuel-air ratio	Total specific fuel consumption (lb)/(hr) (lb thrust)
						Up-stream (lb/sec)	Down-stream (lb/sec)	Total (lb/sec)			
7	6368	2247	2192	55.07	1454	0.66	0.34	1.00	0.0182	0.0293	2.581
8	6836	2644	2532	60.95	1472	.65	.34	.99	.0163	.0278	2.306
9	7480	3192	3044	68.16	1510	.64	.34	.98	.0144	.0268	2.062
10	6354	2557	2325	54.81	1508	.52	1.00	1.52	.0278	.0396	3.052
11	6832	2987	2694	61.29	1525	.52	1.00	1.52	.0248	.0370	2.736
12	7466	3610	3246	68.33	1576	.52	1.00	1.52	.0222	.0354	2.410
13	6329	2757	2442	54.58	1566	.76	.76	1.52	.0278	.0403	2.869
14	6825	3291	2860	61.08	1586	.76	.76	1.52	.0248	.0378	2.528
15	7456	3985	3490	68.14	1647	.78	.74	1.52	.0223	.0365	2.248
16	6319	2817	2463	54.26	1581	.99	.50	1.49	.0275	.0401	2.783
17	6842	3381	2903	61.44	1598	.98	.50	1.48	.0241	.0373	2.437
18	7463	3974	3472	68.45	1651	.97	.49	1.46	.0214	.0355	2.199
22	6369	2776	2334	55.01	1540	1.00	1.01	2.01	.0365	.0483	3.447
23	6848	3295	2712	61.21	1551	1.00	1.01	2.01	.0328	.0451	3.018
24	7500	3983	3323	68.39	1605	1.00	1.01	2.01	.0294	.0429	2.651
26	6840	3295	2712	61.47	1552	1.30	.82	2.02	.0327	.0450	3.021
27	7497	4005	3302	68.68	1609	1.19	.82	2.01	.0292	.0425	2.626
28	6909	3394	2747	61.92	1562	1.01	1.49	2.50	.0403	.0526	3.456
29	7512	4127	3342	68.68	1618	1.00	1.47	2.47	.0359	.0495	2.963
30	6870	3477	2742	61.48	1570	1.26	1.26	2.52	.0408	.0532	3.389
31	7506	4214	3362	68.68	1632	1.25	1.25	2.50	.0364	.0500	2.933
34	7460	4193	3349	69.01	1597	.76	2.19	2.95	.0427	.0562	3.331

National Advisory Committee
for Aeronautics

218-721

NACA RM No. E6J21

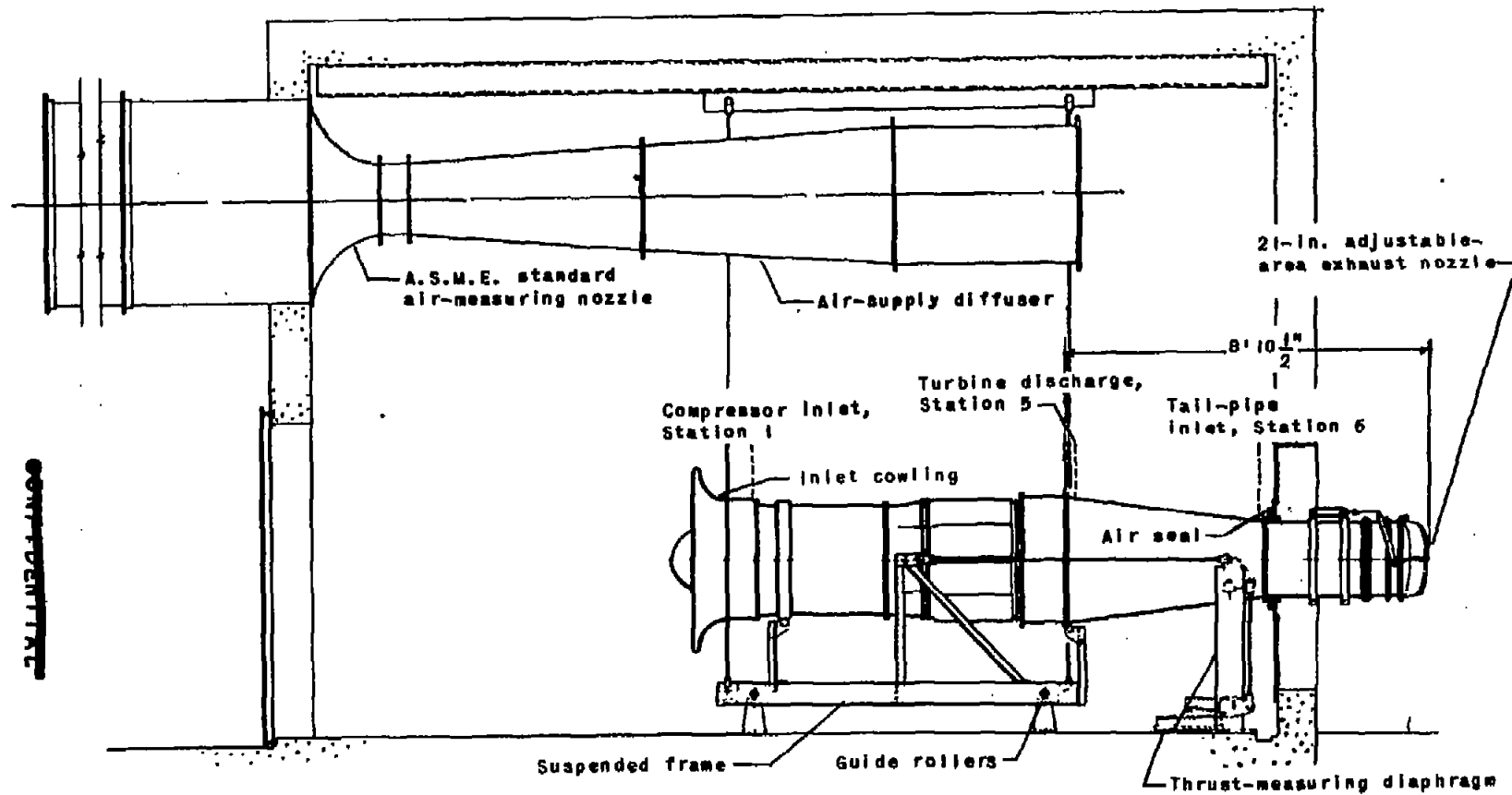


Figure 1. - Schematic diagram of installation of engine with standard tail pipe showing instrumentation stations.

NATIONAL ADVISORY
COMMITTEE FOR AERONAUTICS.

Fig. 1

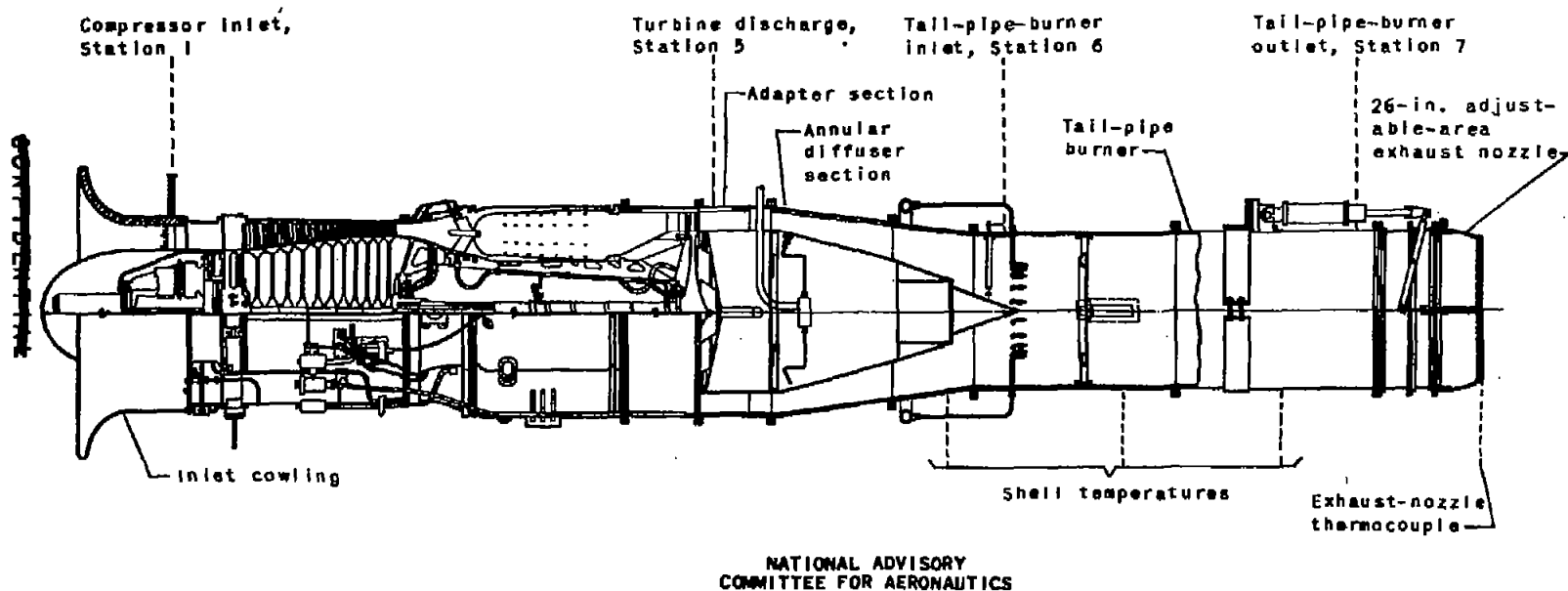


Figure 2. - Turbojet engine with tail-pipe burner showing instrumentation stations.

NATIONAL ADVISORY
COMMITTEE FOR AERONAUTICS

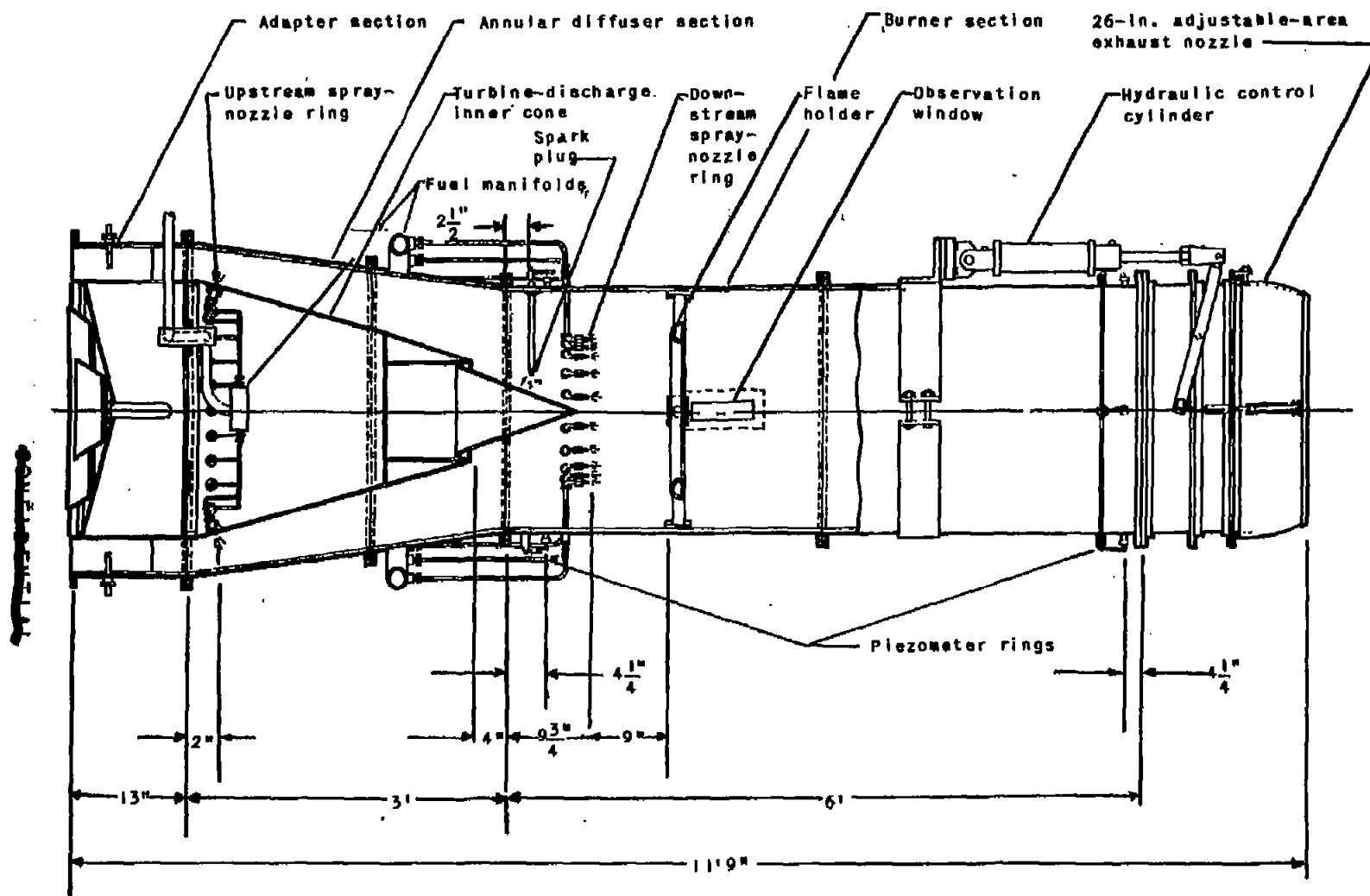


Figure 3. - Sketch of tail-pipe burner for turbojet engine.

NACA RM No. E6J21

FIG. 3

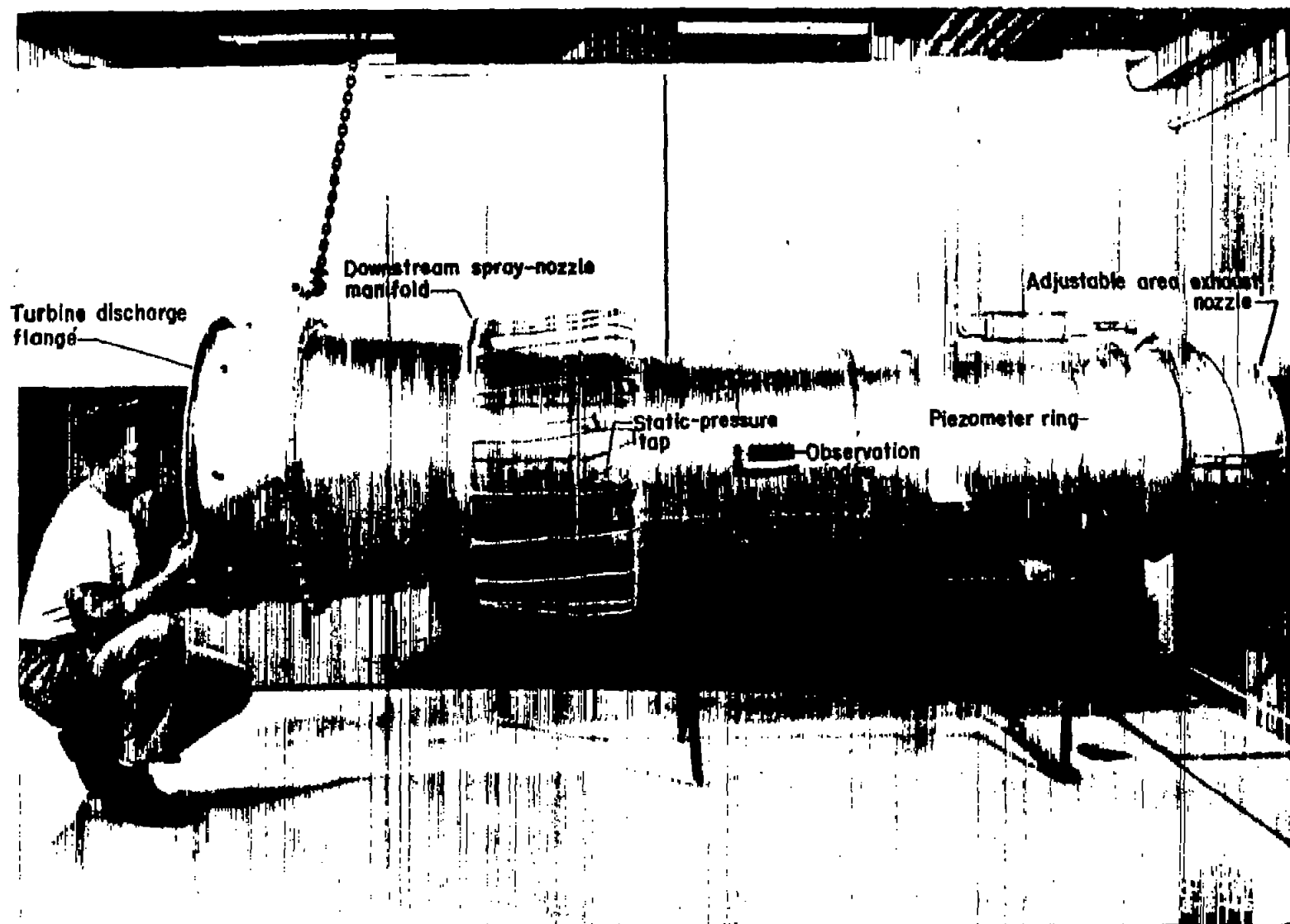


Figure 4. - View of completely assembled tail-pipe burner for turbojet engine.



Figure 5. - View of adapter section and turbine-discharge inner cone for tail-pipe burner showing upstream spray nozzles and step in inner cone.

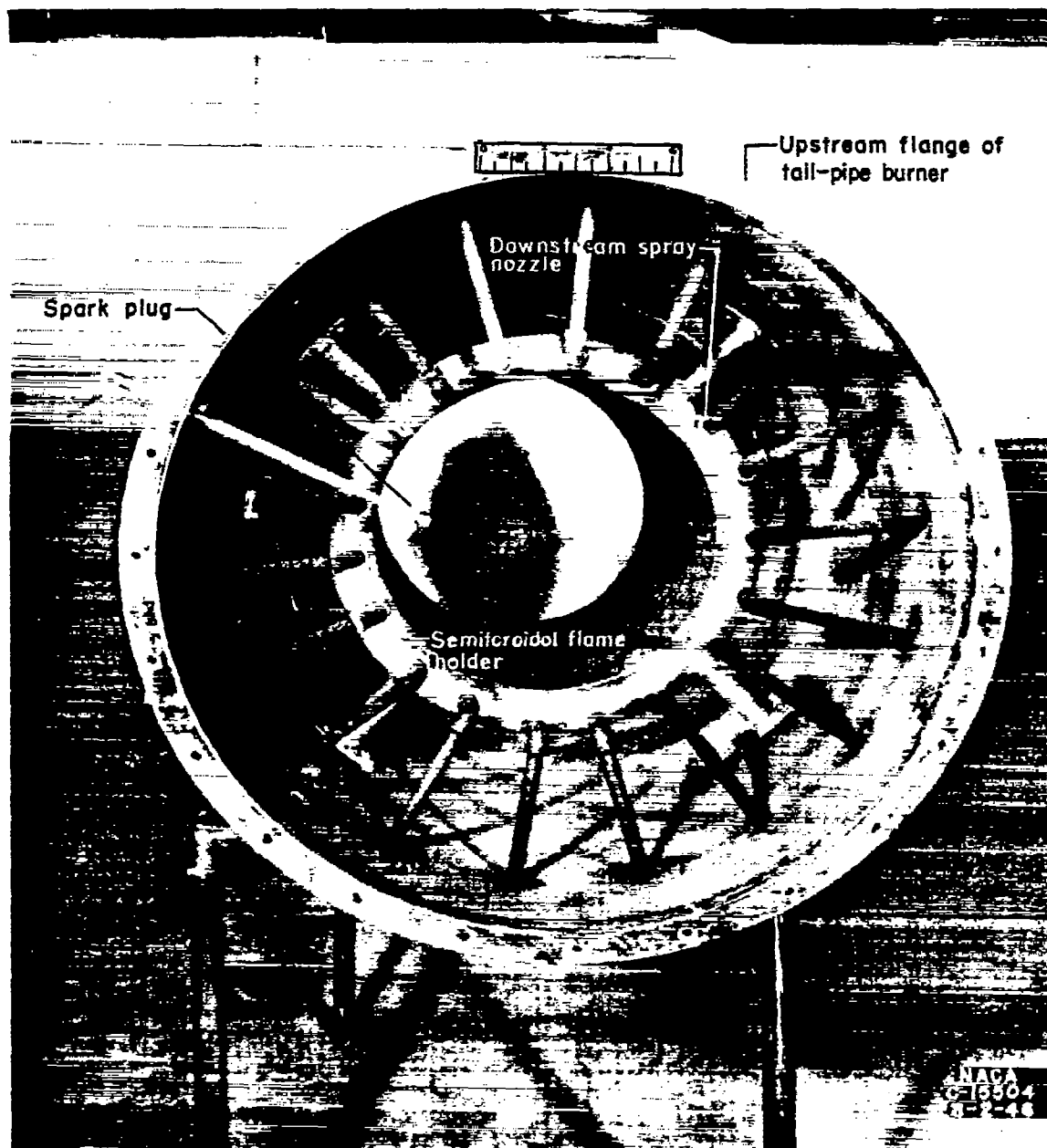


Figure 6. - Upstream view of tail-pipe burner showing downstream spray nozzles and flame holder.

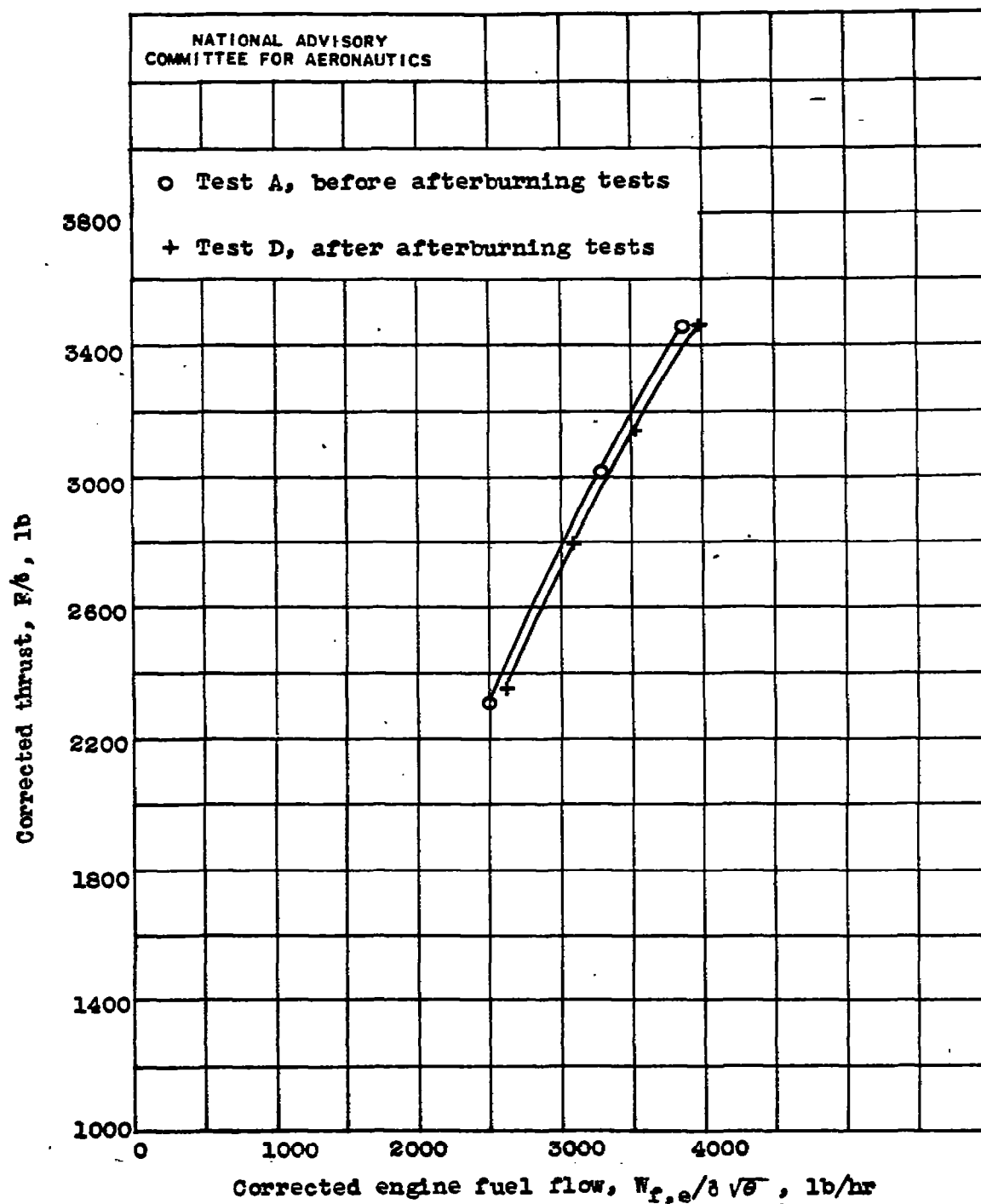
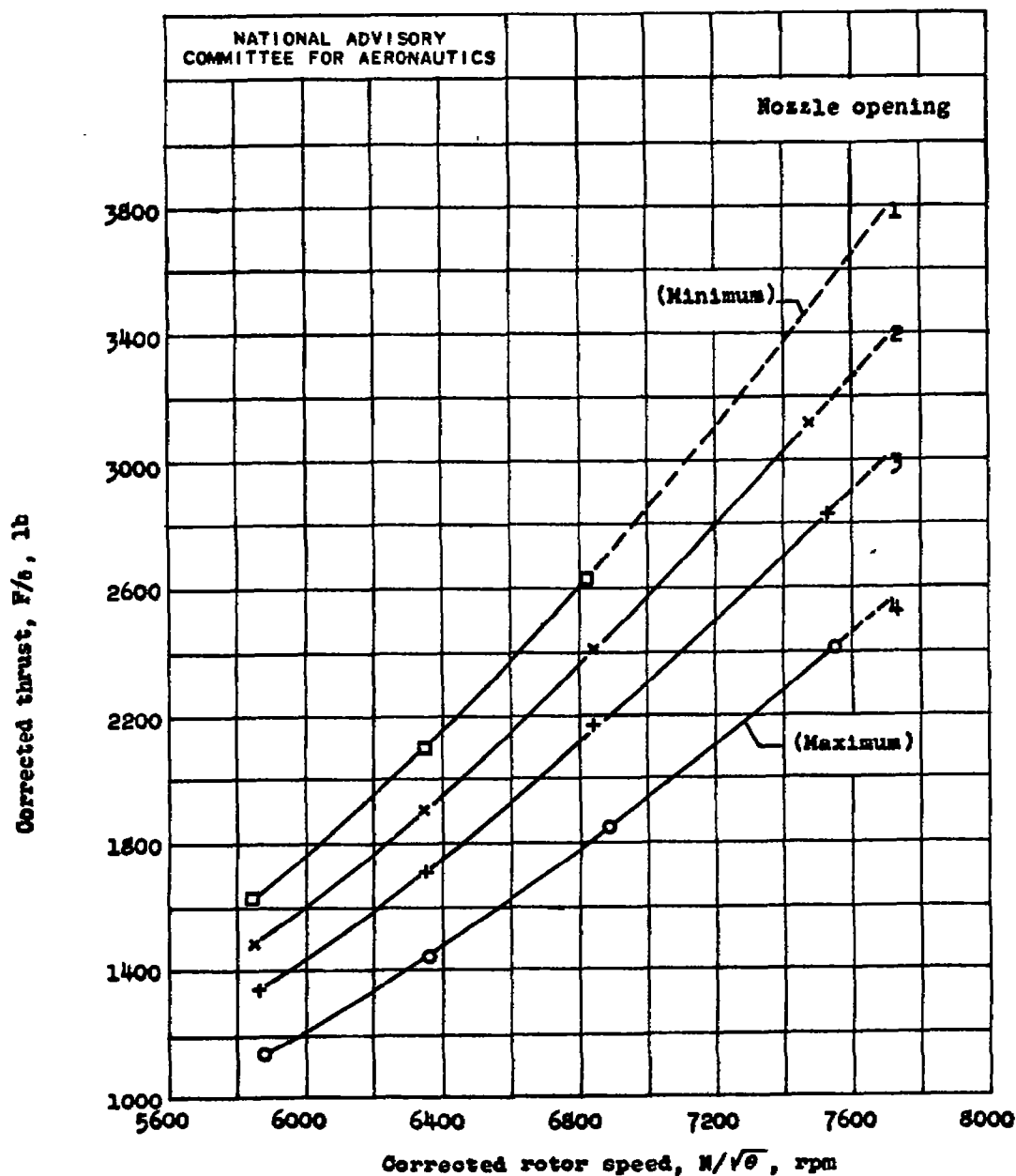
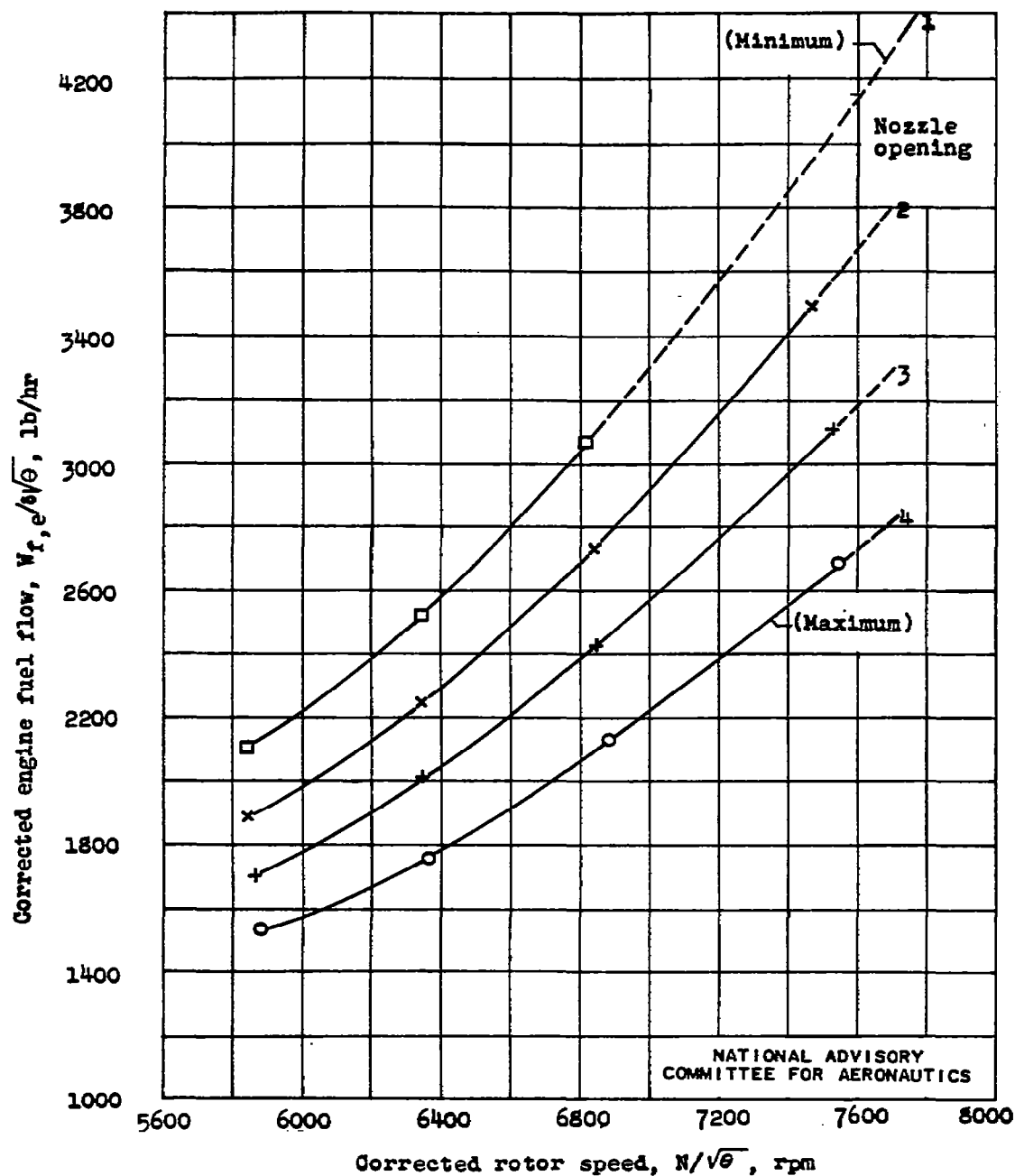


Figure 7. - Comparison of thrust for engine with standard tail pipe from tests A and D at corrected rotor speed of 7500 rpm.



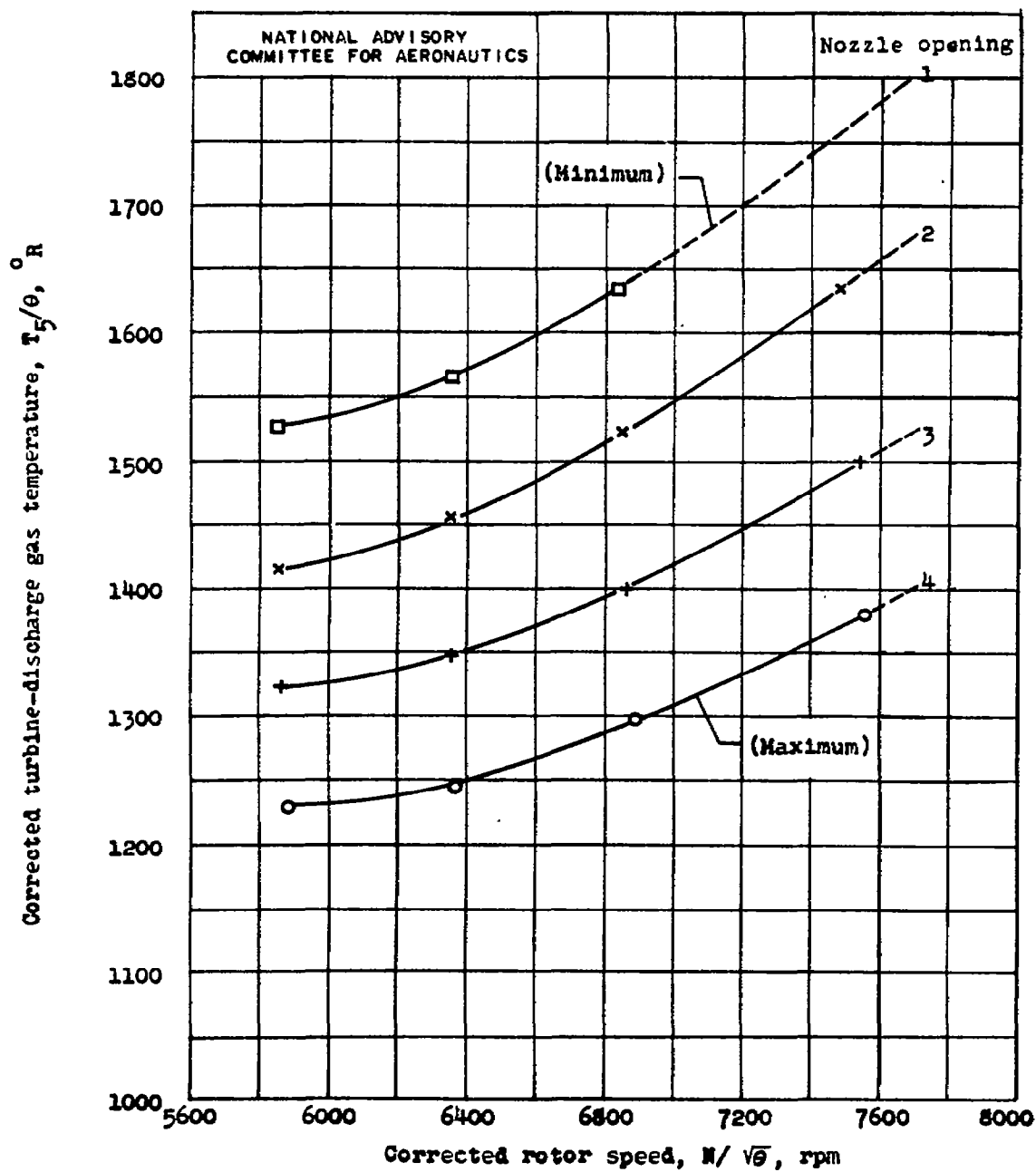
(a) Thrust.

Figure 8. - Performance of engine with standard tail pipe for four positions of adjustable nozzle obtained in test D.



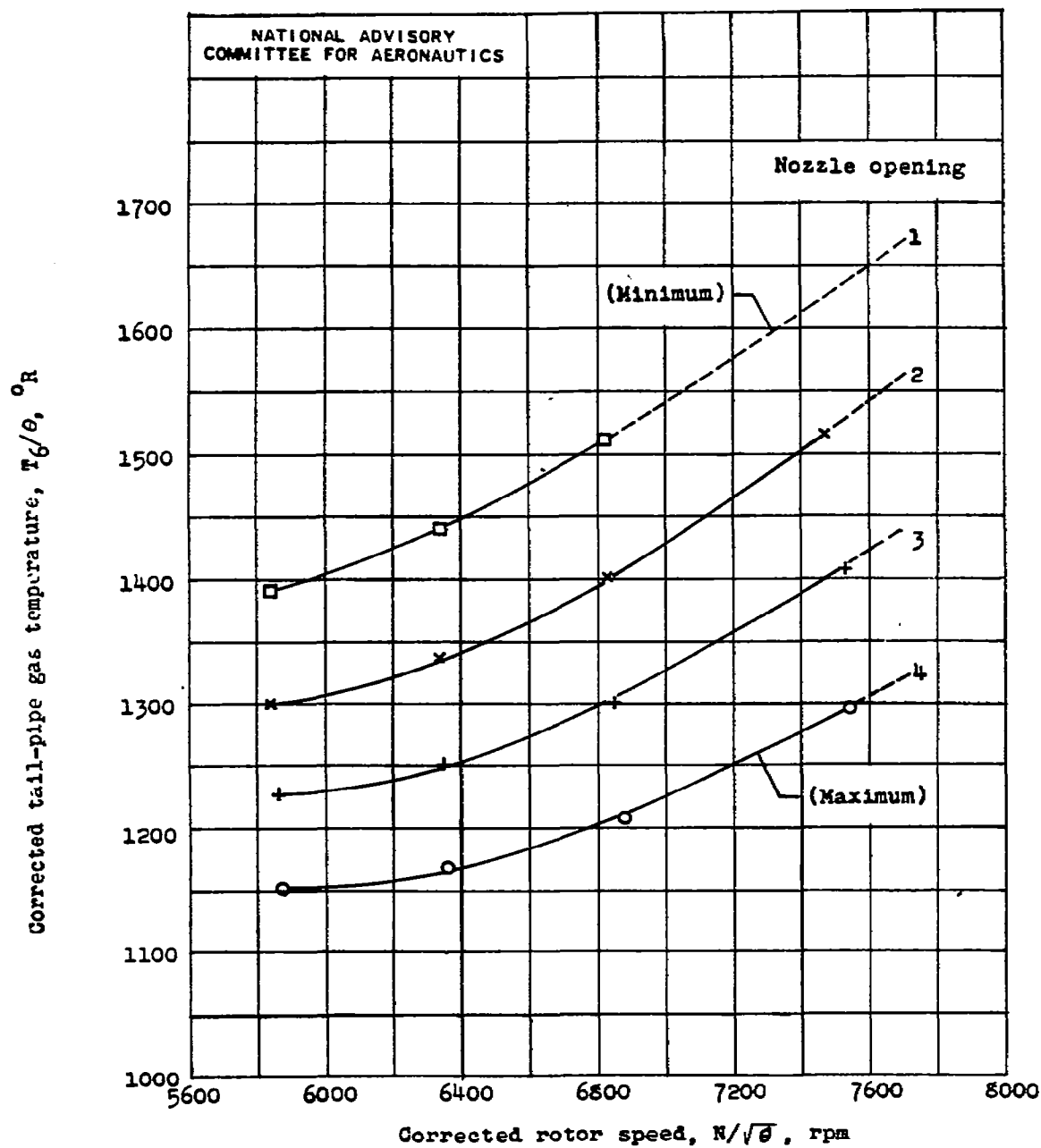
(b) Fuel flow.

Figure 8. - Continued. Performance of engine with standard tail pipe for four positions of adjustable nozzle obtained in test D.



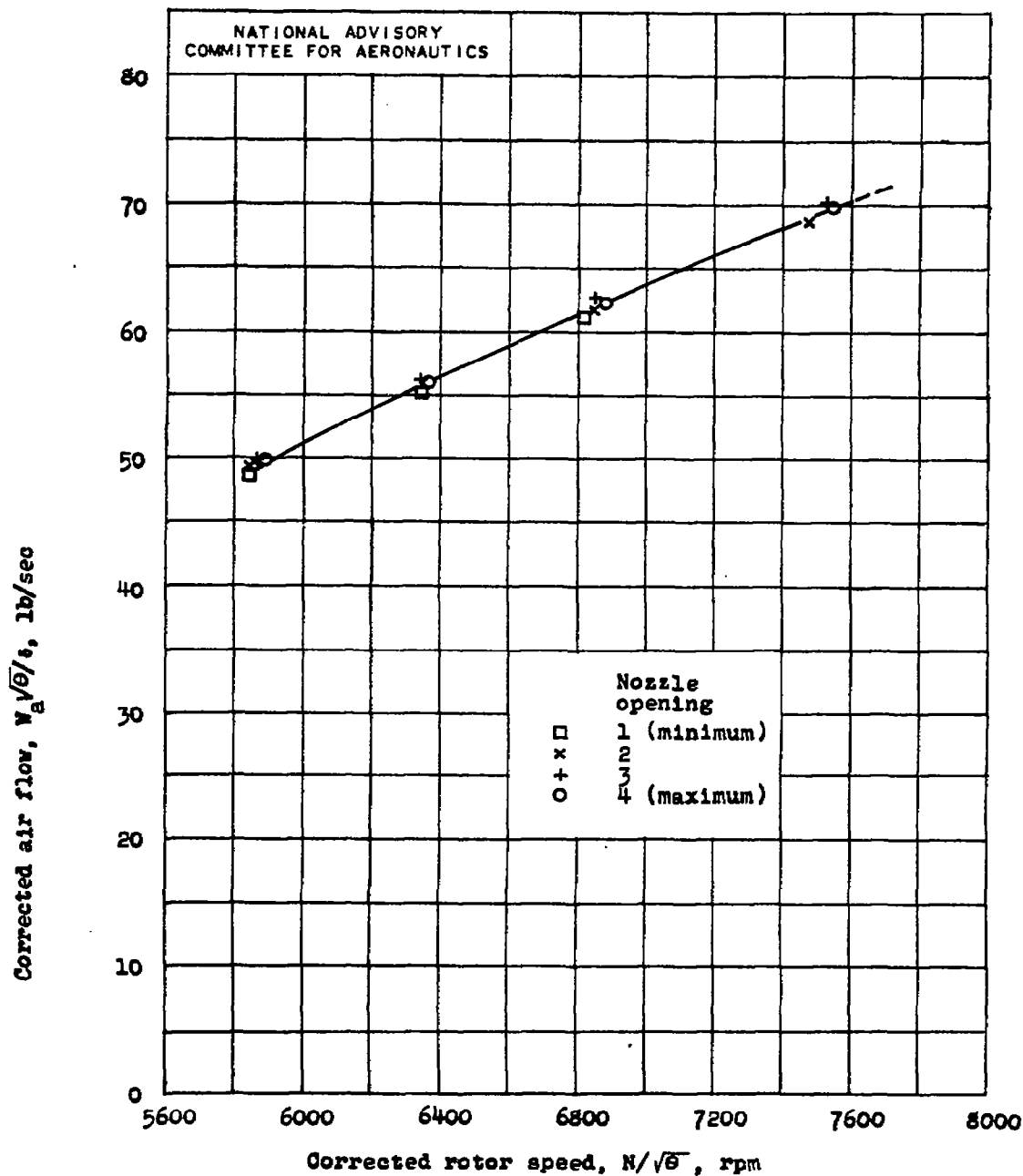
(c) Turbine-discharge gas temperature.

Figure 8. - Continued. Performance of engine with standard tail pipe for four positions of adjustable nozzle obtained in test D.



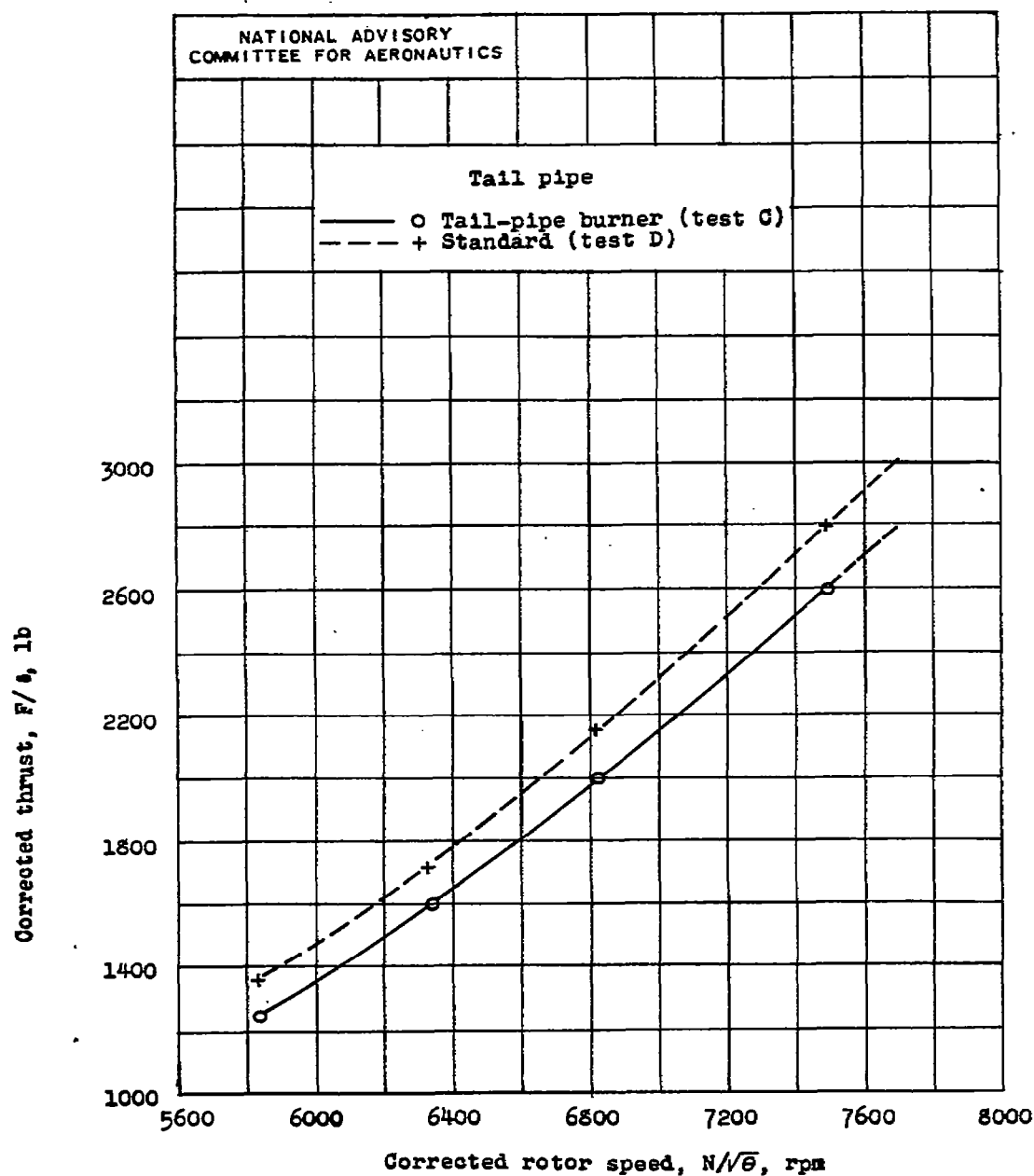
(d) Tail-pipe gas temperature.

Figure 8. - Continued. Performance of engine with standard tail pipe for four positions of adjustable nozzle obtained in test D.



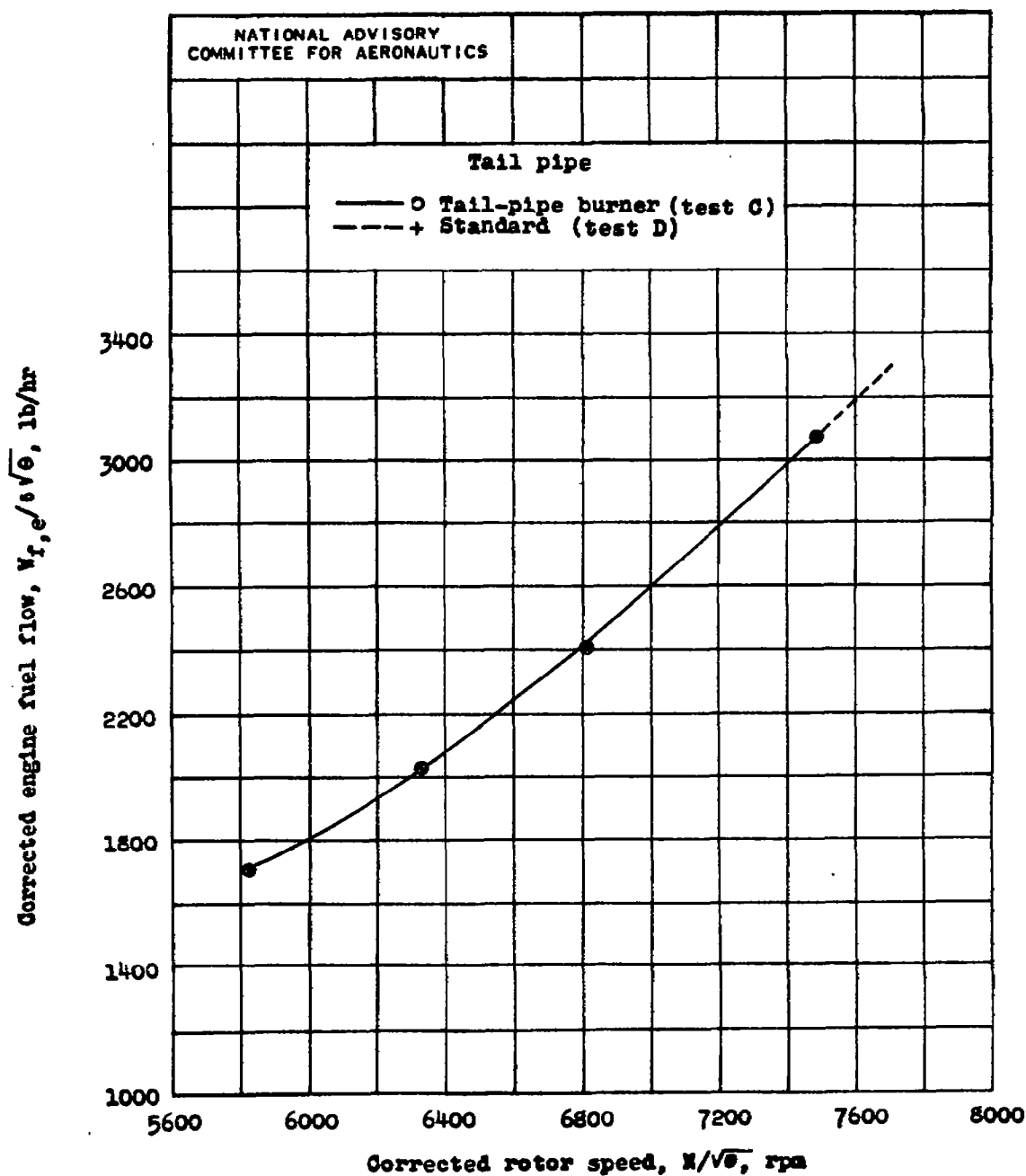
(e) Air flow.

Figure 8. - Concluded. Performance of engine with standard tail pipe for four positions of adjustable nozzle obtained in test D.



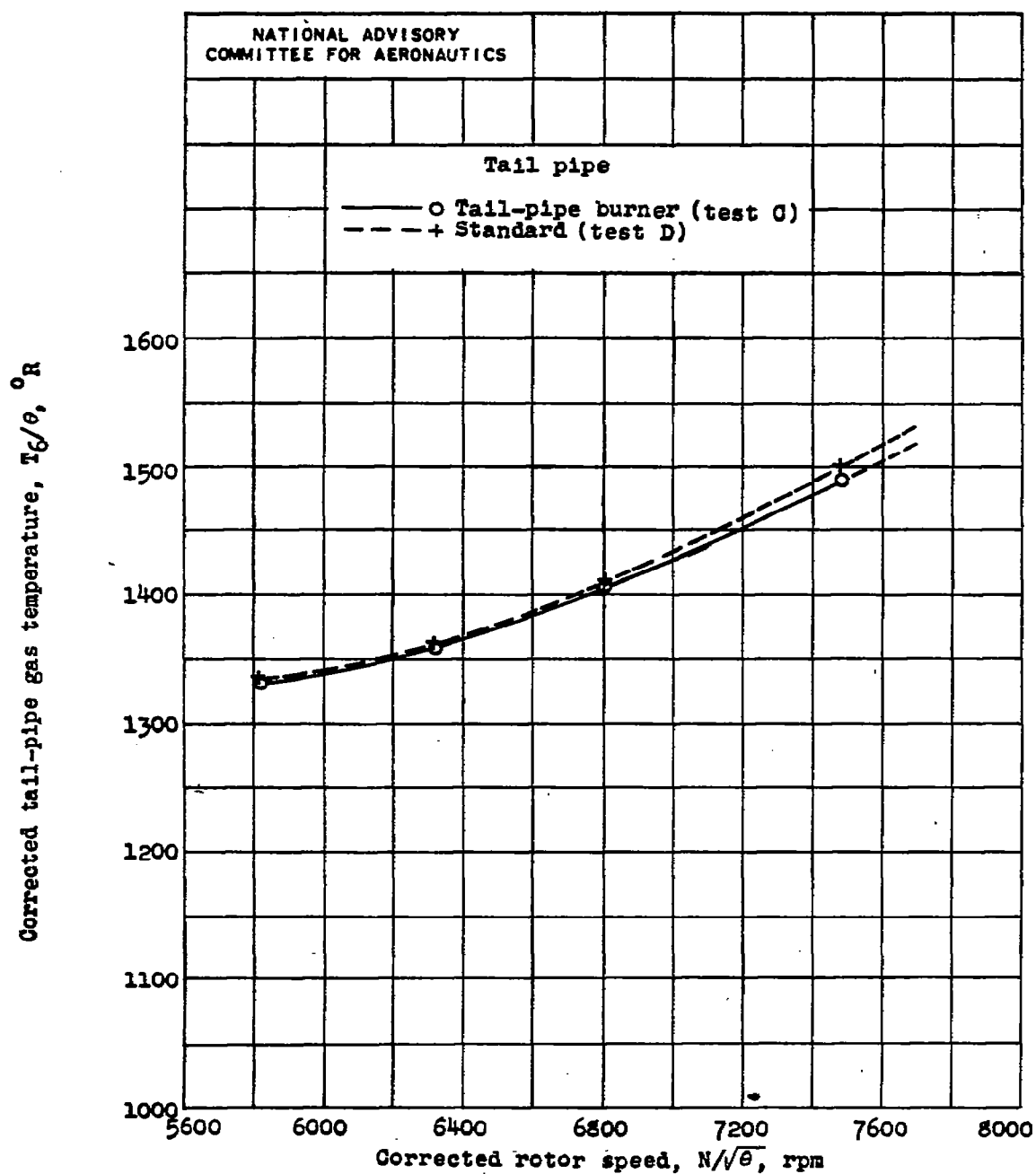
(a) Thrust.

Figure 9. - Comparison of performance of engine with tail-pipe burner (without afterburning) and with standard tail pipe at same engine fuel flows.



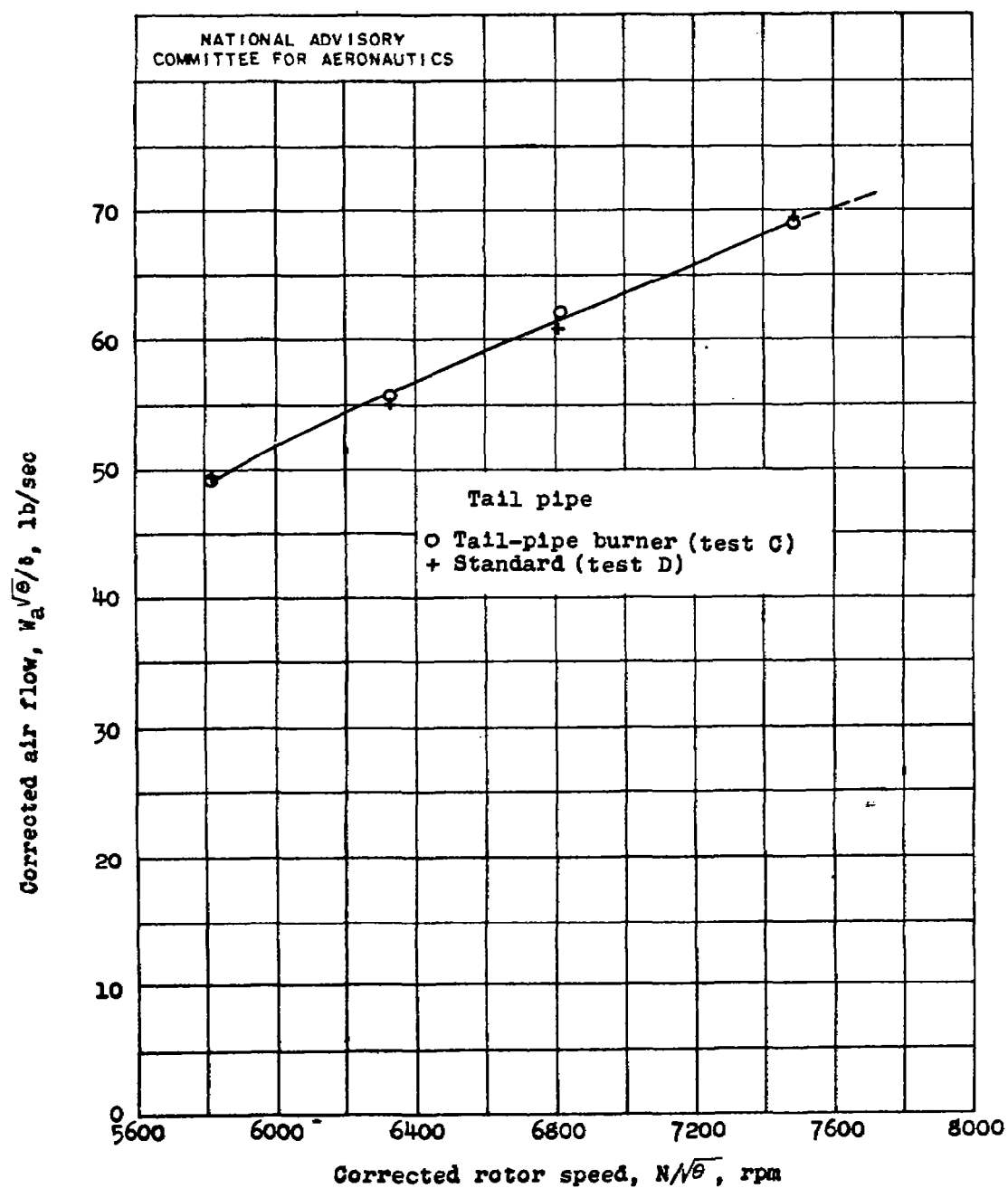
(b) Fuel flow.

Figure 9. - Continued. Comparison of performance of engine with tail-pipe burner (without afterburning) and with standard tail pipe at same engine fuel flows.



(c) Tail-pipe gas temperature.

Figure 9. - Continued. Comparison of performance of engine with tail-pipe burner (without afterburning) and with standard tail pipe at same engine fuel flows.



(d) Air flow.

Figure 9. - Concluded. Comparison of performance of engine with tail-pipe burner (without afterburning) and with standard tail pipe at same engine fuel flows.

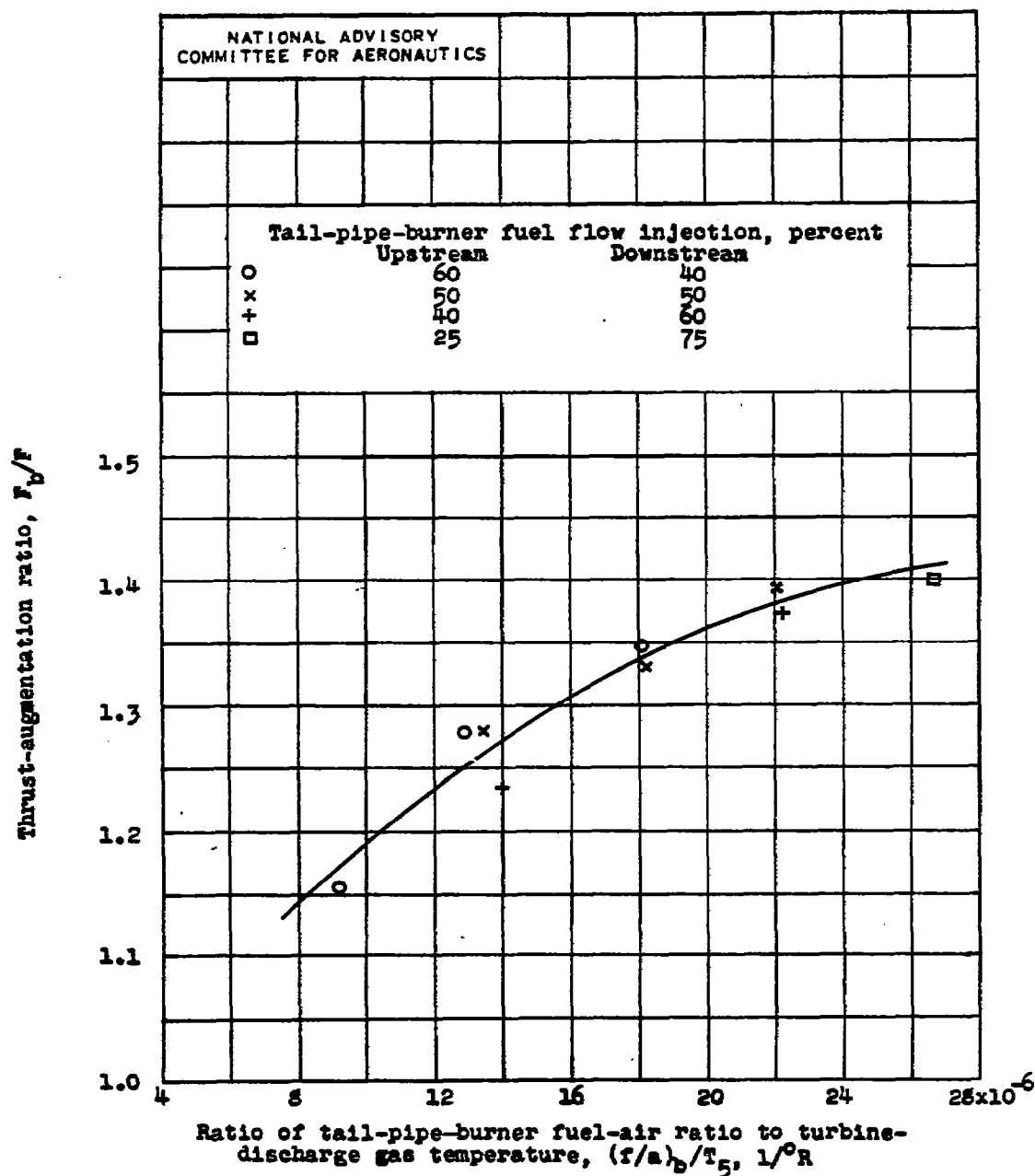


Figure 10. - Variation of thrust augmentation with ratio of tail-pipe-burner fuel-air ratio to turbine-discharge gas temperature at corrected rotor speed of approximately 7500 rpm.

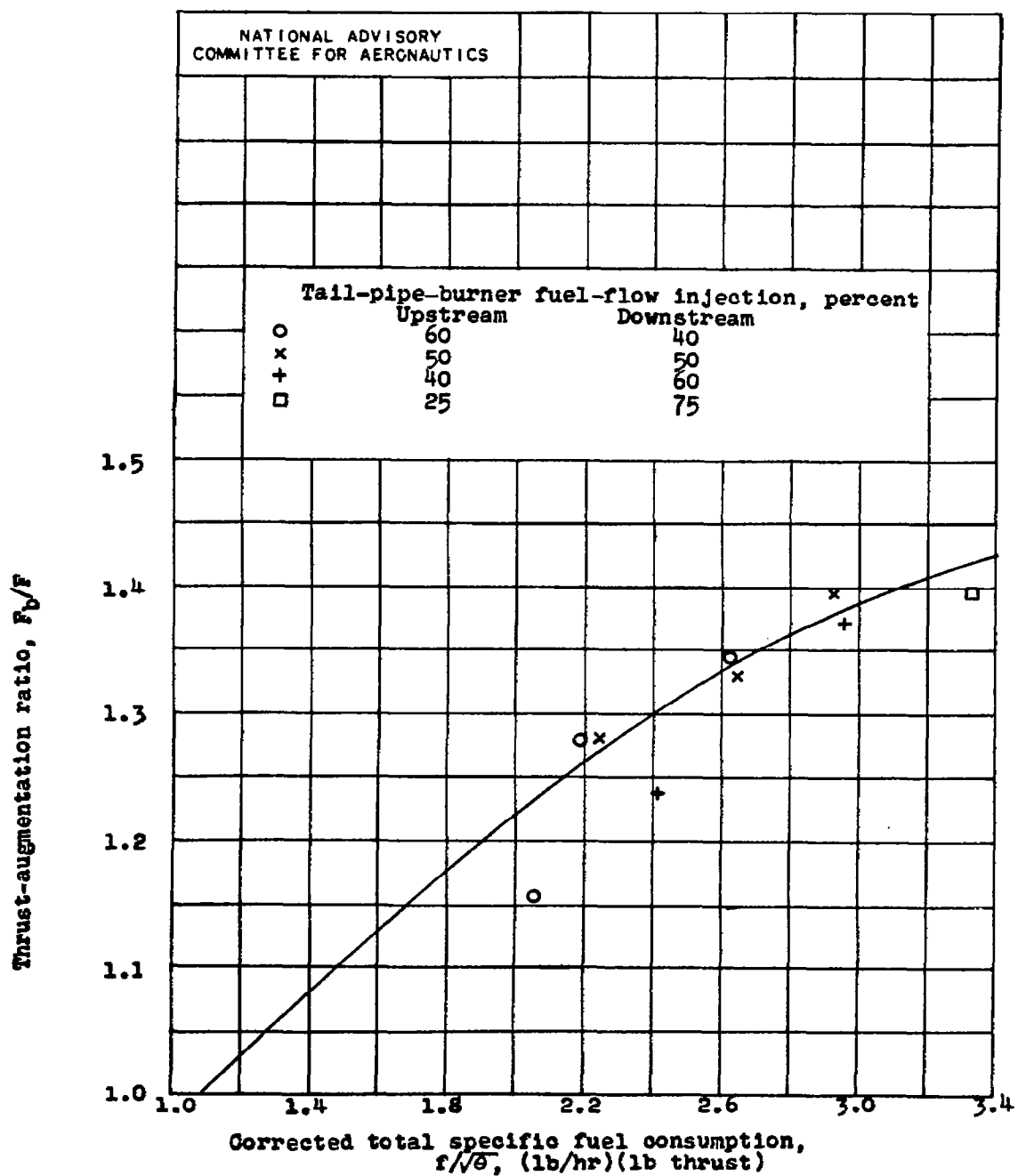


Figure 11. - Variation of thrust augmentation with total specific fuel consumption for corrected rotor speed of approximately 7500 rpm.

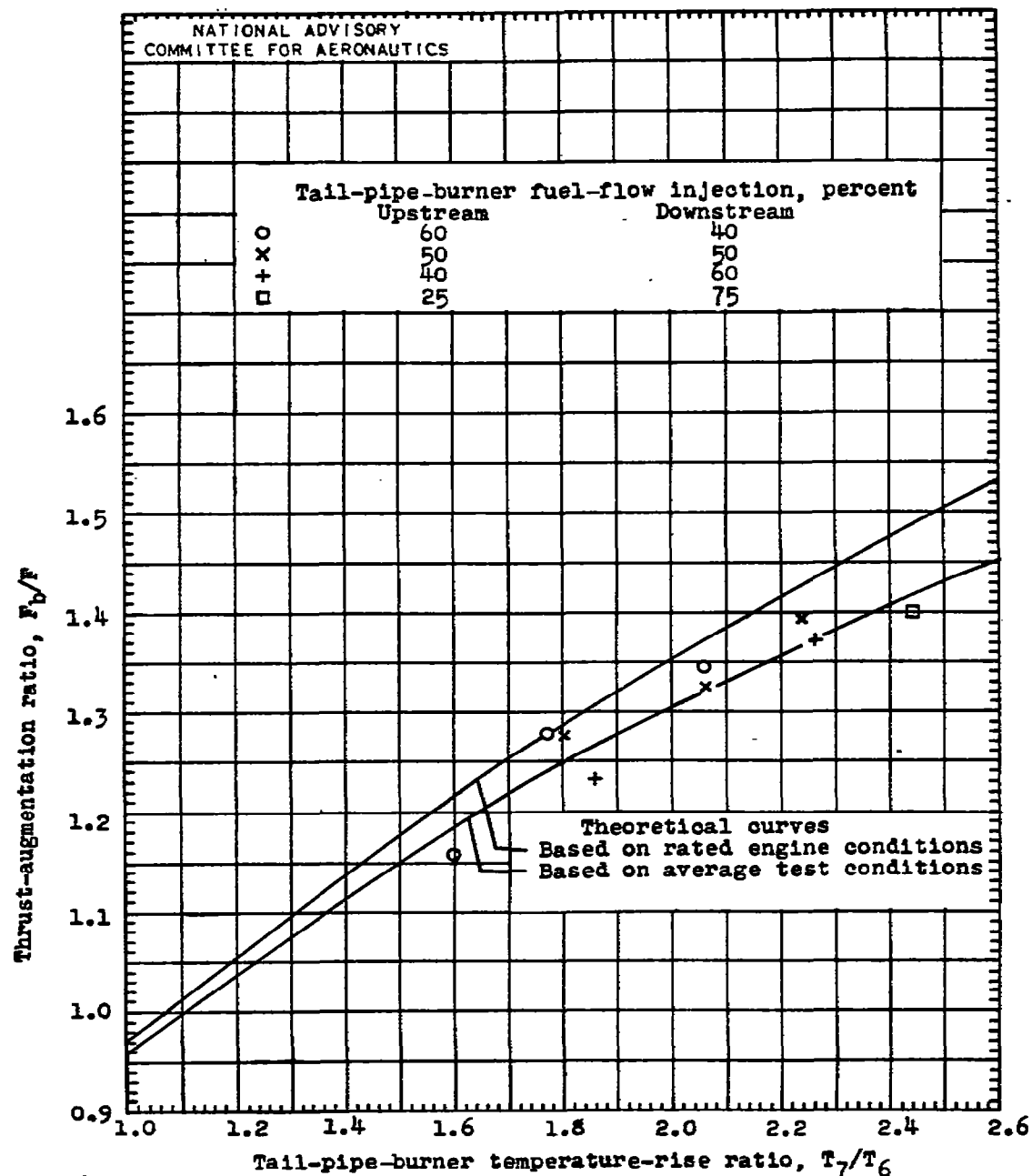


Figure 12. - Variation of thrust augmentation with tail-pipe-burner temperature-rise ratio.

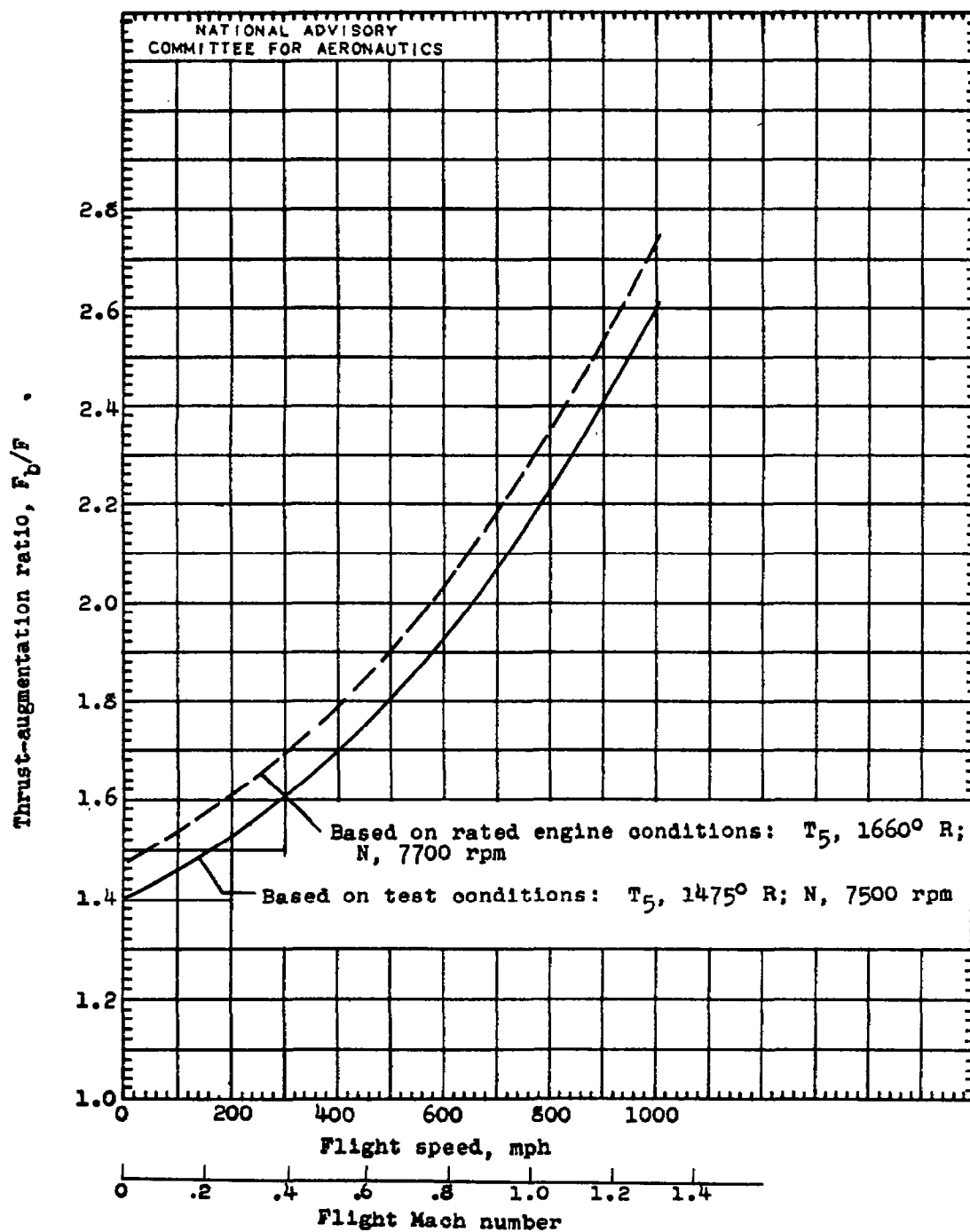
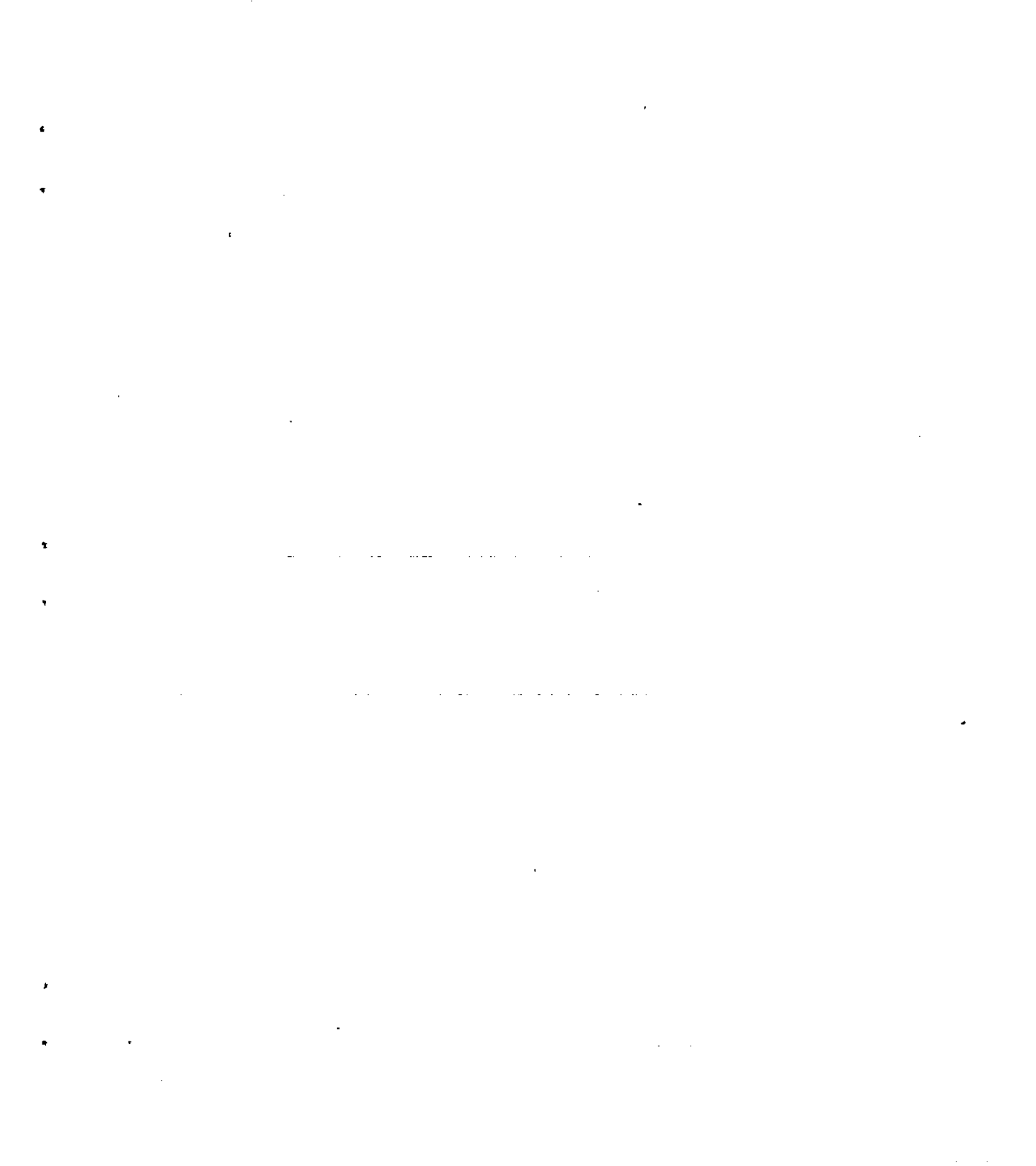


Figure 13. - Variation of calculated thrust augmentation with flight speed for constant turbine-discharge temperature and tail-pipe-burner temperature ratio of 2.34 at sea-level conditions.



NASA Technical Library



3 1176 01435 0327